

Measuring Sweeping Echoes in Rectangular Cross-Section Reverberant Fields

Kenji Kiyohara¹⁾, Ken'ichi Furuya¹⁾, Yoichi Haneda¹⁾, Yutaka Kaneda²⁾

¹⁾ NTT Cyber Space Laboratories, Nippon Telegraph and Telephone Co., 3-9-11 Midori-cho, Musashino-shi, Tokyo 180-8585, Japan. kiyohara.kenji@lab.ntt.co.jp

²⁾ Faculty of Engineering, Tokyo Denki University, 2-2 Kanda-Nishiki-cho, Chiyoda-ku, Tokyo 101-8457, Japan

Summary

We investigated a new acoustical phenomenon, which we call sweeping echoes, in a two-dimensional (2D) space. Sweeping echoes in a three-dimensional (3D) space have recently been reported. We first investigated the regularity of reflected sound in a 2D regularly shaped space based on number theory. The reflected pulse sound train has almost equal intervals between pulses on the squared-time axis as in a 3D space. This regularity of the arrival time of reflected pulse sounds generates sweeping echoes whose frequencies increase linearly with time. Computer simulation of room acoustics shows good agreement with the theoretical results. We first describe our investigation of a square cross-section based on number theory. Next, we describe rectangular cross-sections with various aspect ratios investigated based on the same theory as that for the square. We also discuss our measurements of sweeping echoes in a long hallway. We propose a method for extracting sweep rates of sweeping echoes by calculating their correlation with a time stretched pulse. We analyzed the sweeping echoes for a source and receiver at the center of a rectangular cross-section. These sweeping echoes were not only perceived at the exact center position but also around the center.

PACS no. 43.55.Br, 43.55.Ka, 43.20.El

1. Introduction

A regularly shaped reverberant space often causes specific acoustical phenomena. A handclap (i.e. impulsive sound) between parallel rigid walls yields regular reflected sound pulses on the time axis. This phenomenon is known as a flutter echo [1]. The pulse train, which has constant periods, produces constant frequency sensation.

We recently reported a new echo phenomenon whose frequency increases in proportion to time and named it “sweeping echo” [2]. This phenomenon is caused by the regularity of reflected pulse sounds in a regularly shaped 3D space. This regularity was analyzed using number theory for a cubic reverberant space, and its features are as follows. 1) Most reflected sounds arrive in equal intervals on a squared-time axis, 2) the intervals of reflected sounds decrease in inverse proportion to time, and 3) the fundamental frequency of sweep sounds increases in proportion to time. Since the reflected sounds are perceived as multiple swept sine tones, we named the echo “sweeping echo”. In practice, the echo has been measured in our rectangular parallel-piped reverberation room. This echo can be heard at <http://www.asp.c.dendai.ac.jp/sweep/index.html>.

Thus, in a 3D space, the specific regularity of a reflected sound's arrival time was confirmed theoretically and ex-

perimentally. We focus on the sweep echo phenomenon in a 2D space. Section 2 discusses whether our previously proposed theory [2] can be applied to a 2D space and theoretically analyzes the generation mechanism of the echo. We first discuss a square cross-section and then rectangular cross-sections. Section 2.1 describes the main sweeping echo based on our previous research [2]. From section 2.2, our most recent research is discussed. Section 2.2 describes sub-sweeping echoes in 2D spaces. Section 3 shows simulation results and compares them with the theoretical results. Section 4 shows the experimental results and compares them with the theoretical and simulation results. In Section 5, a new method for detecting sweeping echoes is proposed and the theoretical and experimental results for sweeping echoes are confirmed. Section VI concludes the paper.

We analyzed the sweeping echoes for a source and receiver at the center of a rectangular cross-section. The sweeping echoes were not only perceived at the exact center position but also around the center.

2. Generation mechanism of sweeping echoes

2.1. Main sweeping echo in 2D space

Figure 1 depicts a sound source and its mirror image sources generated in a rectangular cross-section field based on geometrical acoustics [3]. The size of the rectan-

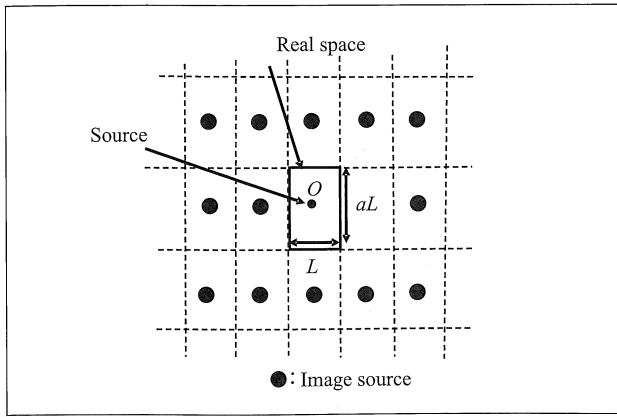


Figure 1. Mirror image sources of rectangular cross-section field. Coordinate origin O set to center of cross-section. Location of each image source represented by $(n_x L, n_y aL)$, where n_x, n_y are positive or negative integers.

gular space is denoted by $L \times aL$, where L and a are real numbers. The reflected sounds can be treated as sounds from the mirror image sources.

The sound source and observation point are located at the center of the rectangular space. The coordinate origin O is also set at the center of the space. The location of each image source is then represented by $(n_x L, n_y aL)$, where n_x and n_y are positive or negative integers. The distance d between the origin and an image source of $(n_x L, n_y aL)$ is represented by

$$d = \sqrt{(n_x L)^2 + (n_y aL)^2} = L \sqrt{n_x^2 + (n_y a)^2}. \quad (1)$$

The arrival time of the sound from the image source is obtained by dividing d by the velocity of sound c , as in

$$t = d/c = \sqrt{n_x^2 + (n_y a)^2} \frac{L}{c}. \quad (2)$$

Next, consider the arrival time on the ‘squared-time axis’, which is derived by squaring equation (2):

$$t^2 = (n_x^2 + (n_y a)^2) \left(\frac{L}{c}\right)^2 = q \left(\frac{L}{c}\right)^2, \quad (3)$$

where

$$q = n_x^2 + (n_y a)^2. \quad (4)$$

If a^2 becomes an integer, q becomes an integer for all n_x and n_y . Now, assume q takes all positive integers when n_x and n_y take all integers; however, this does not happen in actuality, as stated in section 2.2.2. Then, the squared arrival time t^2 in equation (3) has an equal interval $(L/c)^2$.

Considering that a sound source emits a sound pulse, we represent the arrival time of two adjacent pulses (reflected sound) as t_a and t_b ($t_a < t_b$). The interval between these pulses on the squared-time axis is $(L/c)^2$. Namely,

$$t_b^2 - t_a^2 = \left(\frac{L}{c}\right)^2. \quad (5)$$

By factoring the left-hand side of equation (5), we obtain

$$(t_b - t_a)(t_b + t_a) = \left(\frac{L}{c}\right)^2. \quad (6)$$

The mean arrival time t_v of the two pulses is defined by

$$t_v = (t_b + t_a)/2. \quad (7)$$

By substituting equation (7) into equation (6) and modifying the resultant equation, the interval between pulses on the time axis is represented by

$$t_b - t_a = \frac{L^2}{2c^2 t_v}. \quad (8)$$

A periodic pulse series has a fundamental frequency represented by the reciprocal of its interval [4]. Therefore, when the interval of pulses is represented by equation (8), the fundamental frequency of the pulses at time t_v is expressed by

$$f(t_v) = \frac{1}{t_b - t_a} = \frac{2c^2}{L^2} t_v. \quad (9)$$

Equation (9) indicates that the fundamental frequency $f(t_v)$ of the reflected pulse train increases with the arrival time t_v . We call this phenomenon the ‘main sweeping echo’.

For $L = 4$ m, the frequency $f(t_v)$ at $t_v = 1$ s is 14450 Hz with $c = 340$ m/s.

2.2. Sub-sweeping echoes (Effect of forbidden numbers)

Number theory states that q in equation (4) can take the most positive integers but does not take specific positive integer values, which are called ‘forbidden numbers’ [5]. This section describes the effect of these forbidden numbers.

2.2.1. $a = 1$ (Square cross-section)

When $a = 1$ (i.e., a square cross-section), the forbidden numbers are expressed as [6]

$$q \neq k^2 r(4h + 3), \quad (10)$$

where $k, r, h = 0, 1, 2, \dots$ and all squared factors of q are included in k^2 not in $r(4h + 3)$, and $r \neq 4h + 3$.

The forbidden numbers correspond to absent pulses, which are caused by pulses added in anti-phase to all integers. Figure 2(a) shows a pulse series that has completely equal intervals on the squared-time axis, where $L = 4$ m. Figure 2(b) shows an equal amplitude pulse series of a square cross-section field, which lacks pulses due to forbidden numbers. Figure 2(c) shows an anti-phased pulse series corresponding to forbidden numbers, where the amplitudes are normalized as 1. Clearly, Figure 2(a) added to Figure 2(c) becomes Figure 2(b).

For $k = r = 1$, substituting equation (10) into equation (3) gives

$$t^2 = (4h + 3) \left(\frac{L}{c}\right)^2. \quad (11)$$

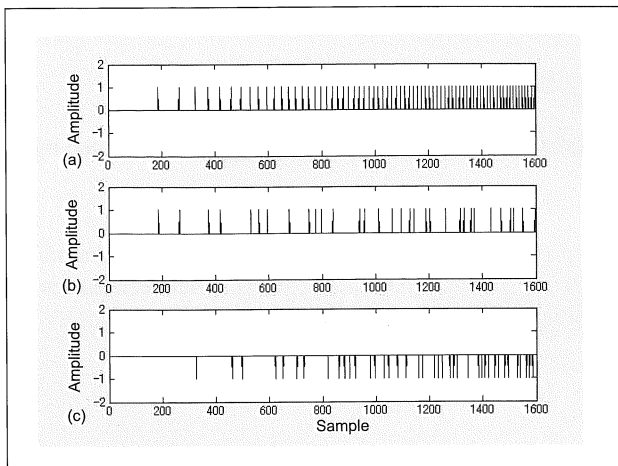


Figure 2. Effect of forbidden numbers. (a) Pulse with completely equal intervals on squared-time axis. (b) Pulse series on time axis of square cross-section for equal amplitudes. (c) Pulse series corresponding to forbidden numbers with negative amplitude of same values. Gaps of (b) are considered to be generated by adding (c) to (a), where dimension L of cross-section was assumed to be 4 m.

Since equation (11) represents pulse arrival times for $h = 0, 1, 2, \dots$, adjacent pulses have interval $4(L/c)^2$ on the squared-time axis. Therefore, the interval of the anti-phased pulse is 4 times longer than that of equation (8), and thus its fundamental frequency is 1/4 that of equation (9), the fundamental frequency of the main sweeping echo. This phenomenon is called “sub-sweeping echo”. For $L = 4$ m, the fundamental frequency of the sub-sweeping echo for $k = r = 1$ at $t_v = 1$ s is 3612 Hz.

Thus, the forbidden numbers cause a regularity in the lack of reflected pulses and this regularity causes sub-sweeping echoes, i.e., echoes with a small frequency sweep rate.

The forbidden numbers indicate that integers are impossible. This means that a reflected sound pulse does not exist at the time corresponding to the forbidden numbers on the squared-time axis.

2.2.2. Forbidden numbers for rectangular cross-section

It is difficult to derive a general solution for forbidden numbers for an arbitrary value of ‘ a ’. Specific forbidden numbers for several values of ‘ a ’ are as follows.

For $a = \sqrt{2}$ in equation (3), q is expressed by

$$q = n_x^2 + 2n_y^2. \quad (12)$$

This q does not have an $(8h + 5)$ - and $(8h + 7)$ -type prime factor [7]. As in the above description, the anti-phased pulse interval is 8-times longer than that of equation (8), so its fundamental frequency becomes 1/8 that of equation (9), i.e., 1806 Hz at 1 s for $L = 4$ m.

Similarly, for $a = \sqrt{3}$, q is calculated with the following equation:

$$q = n_x^2 + 3n_y^2. \quad (13)$$

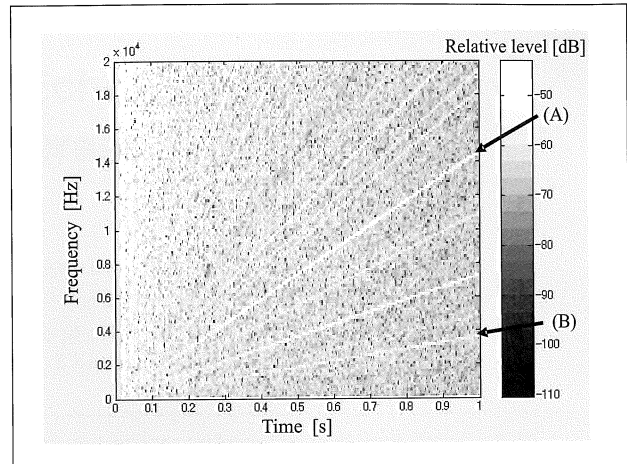


Figure 3. Spectrogram of simulated impulse-response in two-dimensional square space. Multiple sweep sounds can be observed, and main sweeping echo (A) can be clearly observed. Sub-sweeping echo (B) also can be observed.

This q does not have a $(3h + 2)$ -type prime factor [8]. Therefore, the fundamental frequency of the sub-sweeping echo becomes 1/3 of equation (9), i.e., 4816 Hz at 1 s for $L = 4$ m.

For $a = \sqrt{5}$, q is expressed by

$$q = n_x^2 + 5n_y^2. \quad (14)$$

This q does not have a $(20h + 1)$ - and $(20h + 9)$ -type prime factor and $2(20h + 3)$ - and $2(20h + 7)$ -type prime factor [9]. Therefore, the fundamental frequency of the sub-sweeping echo becomes 1/20 that of equation (9), i.e., 722 Hz at 1 s for $L = 4$ m.

The above results are based on number theory; therefore, if a^2 is not an integer, the above theory cannot be applied.

3. Numerical simulation

In this section, we confirm, using numerical simulation, the theoretical results of the sweeping echoes described in section 2.

Echo simulation based on the mirror image method [10] was conducted assuming a 4×4 m 2D space. The band-limited impulse response, or echo series, was calculated by convolving echo pulses with a discrete sinc function. The sampling frequency was 40 kHz. The spectrogram of the impulse response was calculated with a 16-ms Hanning window (62.5-Hz frequency resolution), and the window was shifted in steps of 8 ms.

Figure 3 shows the spectrogram of the impulse response. Multiple sweep sounds, whose frequency components linearly increase with time, can be observed. The main sweeping echo (A) can be clearly observed, and the sub-sweeping echo (B) also can be observed. Other sweeping components are harmonics of the main- and sub-sweeping echoes.

The slopes of lines (A) and (B) in Figure 3 are 14,378 and 3,598 Hz/s, respectively, which are almost consistent with the theoretical values of 14450 and 3612 Hz/s, respectively, calculated above. Thus, the theoretical results discussed in the previous section clearly explain the sweeping echo phenomenon that appeared in the computer simulation of room acoustics.

The theoretical and numerical models are based on the same mirror-images. The good agreement between these models indicates they are essentially the same.

4. Experiment

There are sound spaces that can be regarded as 2D sound spaces. A typical example is a long, straight hallway. A pulse sound generated in such a hallway is reflected repeatedly in the hallway's cross-section, i.e., 2D space. Strictly speaking, the cross-section is not a 2D sound space but a 2D subspace of a 3D sound space. In this subspace, however, the arrival time of the reflected pulses is equivalent to that in a 2D sound space. Therefore, we regard this subspace as a 2D sound space.

However, in practice, 2D sweeping echoes are hardly ever observed, whereas 3D ones can be observed in certain situations. The main reason is that the number of image sources is much smaller in a 2D space than in a 3D space, so the reflected energy is small in a 2D space.

By chance, we found actual sweeping echoes in a hallway at the Tokyo International Forum, at Yurakucho in Tokyo. The cross-section of the hallway is square with 4-m sides, as shown in Figure 4(a). The lateral walls are glass plates, which reflect sound well. The hallway is a 40-m-long straight square pipe, with no junctions or doors except at the end. This seems to be a good example of a 2D sound space.

We measured and analyzed the sweeping echoes generated in this hallway. The measurement conditions are shown in Figure 4(b). The symbols S and R represent the source and receiver positions, respectively. Both source and receiver were located at almost the same height at the center of the hallway. The receiver (microphone) was set behind the source (loudspeaker) for decreasing direct sound.

When a pulse sound (handclap) was generated at position S, sweep sounds whose frequencies increased relatively slowly were perceived, along with ordinary reverberation sounds.

To analyze these sweeping echoes, we recorded impulse response with a microphone placed at position R and a loudspeaker placed at position S emitting a maximum-length (M-)sequence signal. Figure 5 shows the spectrogram of recorded impulse response. The horizontal axis represents time; the time when the pulse sound was generated was set to the origin. The vertical axis represents frequency up to 4 kHz, which was the band within which the sweep sounds were observed. The analysis conditions were as follows: the sampling frequency was 16 kHz, a 256-sample rectangular window was used for discrete

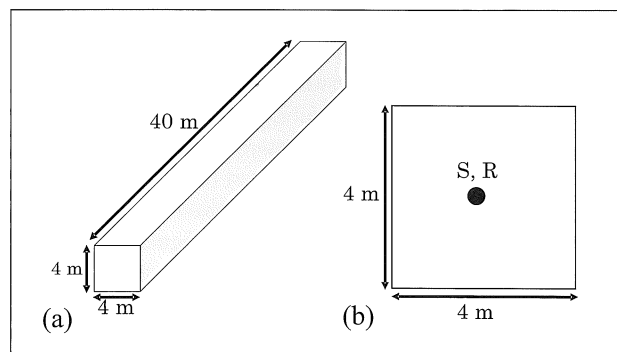


Figure 4. Layout for sweep-sound measurement. (a) Dimensions and (b) cross-section, S: source position; R: receiver position.

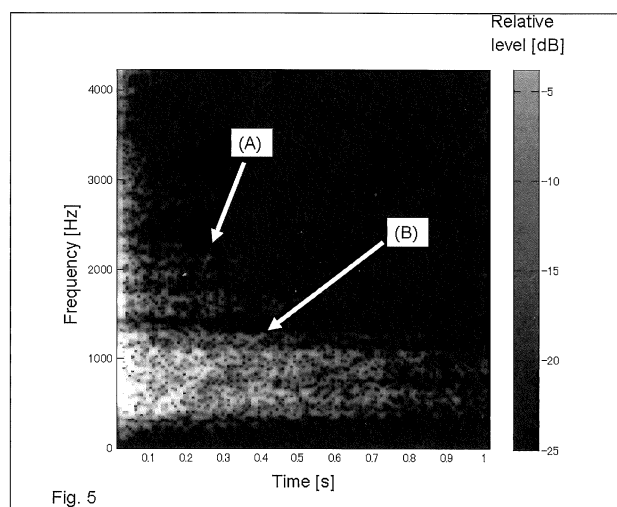


Figure 5. Spectrogram of recorded data. Main sweeping echo (A) vaguely appears from 0 to about 0.2 s. Frequency of main sweeping echo increased linearly with time and increased to about 2200 Hz during first 0.2 s. Following main sweeping echo, sub-sweeping echo (B) also appears with slope of about 3500 Hz/s.

Fourier transform (DFT), and the window was shifted by 128 samples.

In Figure 5, a sub-sweeping echo whose frequency increases linearly with time can be seen (Line B). The slope of the sub-sweeping echo in Figure 5 is about 3500 Hz/s, which is in good agreement with the theoretical 3612 Hz/s calculated by equation (9).

Compared with the simulation results in Figure 3, the sub-sweeping echo in Figure 5 is not clear. There are two main reasons for this lack of clarity. First, the reflection coefficient was set to 1 in the simulation, while the mean pressure reflection coefficient of the experimental space was about 0.9, determined using numerical simulation. Generally, in a real space, the higher the frequency, the lower the reflection coefficient, which means low-frequency reverberance. This causes fast decay of the high-frequency components of sweeping echoes. Sweeping echoes clearly appeared at high frequencies but only vaguely at low frequencies, as shown in the simulation results in Figure 3. Therefore, sweeping echoes were not clear.

Second, there were differences between the ideal and practical spaces. The walls are not perfectly parallel and rigid, and the floor has small uneven bumps to prevent people slipping. Sections of the ceiling are made of perforated metal without sound absorption material, and the diameter of perforation is about 1 cm and open ratio is about 20%; therefore, the ceiling is reflective in low frequencies and absorptive in high frequencies. These irregularities of the space also caused the sweeping echoes to be unclear.

The main sweeping echo scarcely appears in Figure 5. This may be explained by the frequency of the main sweeping echo increasing and decaying quicker than that of the sub-sweeping echo.

5. Method for extracting sweep sound

In the simulation results, sweeping echoes clearly appeared in the spectrograms. However, the sweeping echoes in the measured sound cannot be clearly seen in the spectrogram, as shown in Figure 5. Therefore, we propose a new method for quantitatively extracting sweep-sound components by calculating the correlation with a complex up-sweep sine signal described in the next section.

5.1. Complex ascending sweep sine signal

An ascending sweep sine signal is a sine signal whose frequency increases linearly with time, it is also called a chirp signal. We created the sine signal based on the time stretched pulse (TSP) method [11]. An up-TSP signal (ascending sweep sine wave) is defined in the frequency domain as follows:

$$\text{TSP}(m) = \begin{cases} \exp(-j2M\pi(m/N)^2) & \text{for } 0 \leq m \leq N/2, \\ \text{TSP}(N-m)^* & \text{for } N/2 < m < M, \end{cases} \quad (15)$$

where N is discrete signal length, m is discrete frequency, and $*$ represents the complex conjugate. The parameter M is a length where the sweep sine signal exists in practical terms in all length N . The up-TSP signal $tsp(k)$ (k : discrete time) is obtained by executing inverse fast Fourier transform (FFT) of the $\text{TSP}(m)$.

A spectrogram of the up-TSP signal is shown in Figure 6. The frequency increases from 0 to $f_s/2$ (f_s : sampling frequency) during time M/f_s . Therefore, the increase in frequency in 1 s is inversely proportional to M as

$$\frac{f_s}{2} \Big/ \frac{M}{f_s} = \frac{f_s^2}{2M}. \quad (16)$$

By varying M , it is possible to control the frequency sweep rate of the sweep sine wave.

However, in this form, the phase of the sine wave affects extraction of sweep sound. To avoid this, a complex sine signal is introduced using inverse FFT of the following

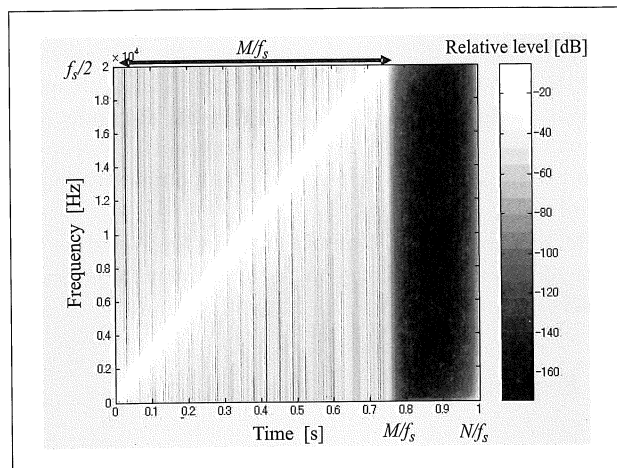


Figure 6. Spectrogram of TSP signal.

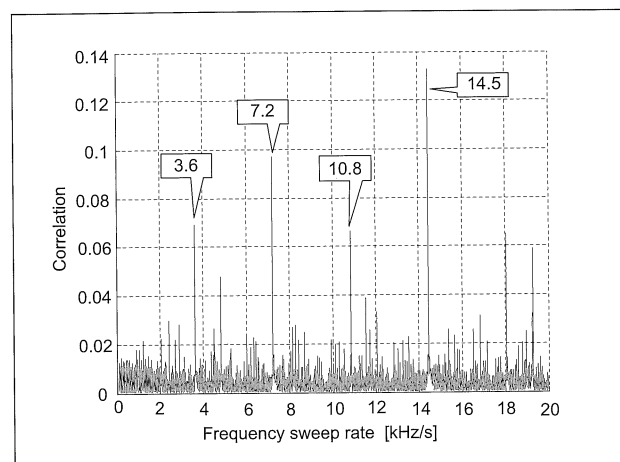


Figure 7. Correlation of simulated data with conjugated complex ascending sweep sine (CCASS) signal. Main sweeping echo (14.5 kHz/s) and sub-sweeping echo (3.6 kHz/s) are clear.

equation, where negative-frequency components are zero in equation (15):

$$\text{CCASS}(m) = \begin{cases} \exp(-j2M\pi(m/N)^2) & \text{for } 0 \leq m \leq N/2, \\ 0 & \text{for } N/2 < m < M. \end{cases} \quad (17)$$

It seems possible to extract sweep signal components of a sound by calculating correlations of the objective sound with the varying frequency sweep rate of a conjugated complex ascending sweep sine (CCASS) signal as described above.

5.2. Correlation results with sweeping echoes

We calculated the correlation of the CCASS signal with the simulation and measured data. The results are shown in Figures 7 and 8, respectively. In these figures, the horizontal axis indicates the frequency sweep rate [kHz/s] of the CCASS signal, and the vertical axis indicates the normalized cross-correlation value.

As shown in Figure 7, sharp peaks appear at around 3.6 and 14.5 kHz/s, corresponding to the frequency sweep

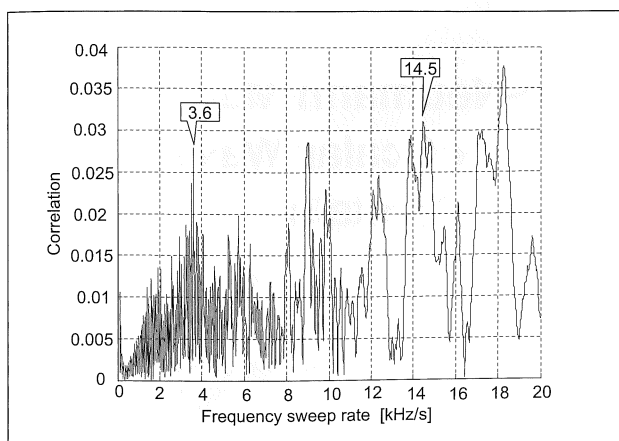


Figure 8. Correlation of measured data with CCASS signal. Main sweeping echo (14.5 kHz/s) and sub-sweeping echo (3.6 kHz/s) are clear, as in Figure 7.

rate of the sub- and main-sweeping echo, respectively, of the simulated data, as described in Section III. The peaks at around 7.2 and 10.8 kHz/s are harmonics of the sub-sweeping echo. The detected results in Figure 7 indicate good agreement with the frequency sweep rate of each sweeping component in Figure 3. Therefore, we confirmed the validity of the proposed analyzing method.

The analyzed results for the measured data are shown in Figure 8. A clear peak appears around 3.6 kHz, confirming the existence of a sub-sweeping echo. The peak is at maximum in components below 8 kHz/s. Contrary to the results with the simulated data, the measured data harmonics cannot clearly be observed.

The main sweeping echo can be confirmed because a peak exists around 14.5 kHz. However, many peaks are observed at large frequency sweep rates (ex. over 8 kHz/s). The reason is that the total length of the sweep is short when the frequency sweep rate is large, so the length of correlation is short, namely the sweep starts to decay soon after the start of measurement. This causes the early strong component in the measured data, which is not necessarily the sweep sine component, to affect the correlation value. Thus, the calculated values seemed to vary widely.

As described above, the sub-sweeping echo in an actual 2D space observed only vaguely in a spectrogram can be detected with the proposed method. Thus, from this vague spectrogram, theoretical sweep sounds can be detected.

6. Conclusion

We investigated the regularity of reflected pulse sounds in a 2D space based on number theory. We found that the arrival times of the pulse sounds from mirror image sources in a rectangular space have almost equal intervals on the squared-time axis. This regularity of the pulse intervals generates a “main sweeping echo”, whose frequency component linearly increases with time. The reflected pulse train, however, does not have completely

equal intervals on the squared-time axis; there are missing pulses corresponding to “forbidden numbers” based on number theory. These missing pulses were found to have relatively long, equal intervals. This regularity causes “sub-sweeping echoes”, whose frequency components increase slowly.

Computer simulation based on the mirror image method showed both main- and sub-sweeping echoes. The sweeping speeds of these echoes agreed well with the theoretical results.

The regularities of reflected sounds in a 2D space are similar to those in a 3D sound space, but the number of image sources is much smaller in a 2D space than in a 3D space. Thus, the reflected energy is small in a 2D space, which is why sweeping echoes are rarely perceived there. However, we observed sweeping echoes in an actual long hallway with a square cross-section. The frequency sweep rate of the observed sub-sweeping echo corresponded well to the theoretical and simulated results.

Finally, we proposed a method for extracting sweep sound components, which uses CCASS (conjugated complex ascending sweep sine). By changing the frequency sweep rate of the CCASS signal, correlation is calculated with an objective signal. The correlation with a simulated room’s impulse response confirms the validity of the proposed method. The correlation with a real space’s impulse response clearly shows the existence of a sub-sweeping echo, which could not be clearly observed in the spectrogram.

Acknowledgement

We thank Mr. Haruhiko Kojima of NTT (Nippon Telegraph and Telephone Co.) for supporting our work.

References

- [1] H. Kuttruff: Room acoustics. Elsevier Applied Science, London and New York, 1991. 81.
- [2] K. Kiyohara, K. Furuya, Y. Kaneda: Sweeping echoes perceived in a regularly shaped reverberation room. *J. Acoust. Soc. Am.* **111** (2002) 925–930.
- [3] Reference 1 pp. 81–95.
- [4] A. Papoulis: The Fourier integral and its application. McGraw-Hill, New York, 1962. 43–44.
- [5] M. R. Schroeder: Number theory in science and communication. Springer-Verlag, New York, 1984. 98.
- [6] P. G. L. Dirichlet, R. Dedekind: Lectures on number theory. Amer. Mathematical Society, 1999. 68.
- [7] Reference 6 §69.
- [8] Reference 6 §70.
- [9] Reference 6 §71.
- [10] J. B. Allen, D. A. Berkley: Image method for efficiently simulating small-room acoustics. *J. Acoust. Soc. Am.* **65** (1979) 943–950.
- [11] Y. Suzuki, F. Asano, H. Y. Kim, T. Sone: An optimum computer-generated pulse signal suitable for the measurement of very long impulse responses. *J. Acoust. Soc. Am.* **97** (1995) 1119.